Sophoricoside attenuates autoimmune-mediated liver injury through the regulation of oxidative stress and the NF-κB signaling pathway

YU CHEN, YU LEI, HAN WANG, LIJIA WANG, JIAXIN XU, SHUHUI WANG, MEIPING YU, ZHANGQI PENG, FANG XIAO, DEAN TIAN and MEI LIU

Department of Gastroenterology, Tongji Hospital of Tongji Medical College, Huazhong University of Science and Technology, Wuhan, Hubei 430030, P.R. China

Received April 25, 2023; Accepted July 4, 2023

DOI: 10.3892/ijmm.2023.5281

Abstract. The prevalence of autoimmune hepatitis (AIH) is increasing, yet specific pharmacotherapies remain to be explored. The present study aimed to investigate the effects of sophoricoside (SOP), a bioactive component of medical herbs, on AIH and to elucidate the underlying mechanisms. Bioinformatic approaches were used to predict the potential targets and underlying regulatory mechanisms of SOP on AIH. The effects of SOP on AIH were evaluated by determining the expression levels of inflammatory cytokines, histological liver injury and hepatic fibrosis in an improved chronic cytochrome P450 2D6 (CYP2D6)-AIH mouse model and in a model of concanavalin-A (ConA)-induced acute immune-mediated liver injury. The antioxidant activity of SOP was detected in *in vivo* and *in vitro* experiments. The selected signal targeted by SOP in AIH was further confirmed using western blot analysis and immunofluorescence staining. The results of bioinformatic analysis revealed that the targets of SOP in AIH were related to oxidative stress and the NF-κB gene set. The NF-κB transcription factor family is a key player that controls both innate and adaptive immunity. The activation of the NF-κB signaling pathway is often associated with autoimmune disorders. In the animal experiments, SOP attenuated CYP2D6/ConA-induced AIH, as evidenced by a significant reduction in the levels of hepatic enzymes in serum, inflammatory cytokine expression and histological lesions in the liver. The oxidative response in AIH was also significantly inhibited by SOP, as evidenced by a decrease in the levels of hepatic malondialdehyde, and elevations in the total antioxidant capacity and glutathione peroxidase levels. The results of the *in vivo* and *in vitro* experiments revealed that SOP significantly reduced the enhanced expression and nuclear translocation of phosphorylated p65 NF-κB in the livers of mice with AIH and in lipopolysaccharide-stimulated AML12 cells. On the whole, the present study demonstrates the protective role of SOP in AIH, which may be mediated by limiting the oxidative response and the activation of the NF-κB signaling pathway in hepatocytes.

Introduction

Autoimmune hepatitis (AIH) is a type of chronic progressive liver disease and has recently exhibited a global increasing trend in incidence (1,2). Immune-mediated injury to hepatocytes is the major pathophysiological feature of AIH, which is pivotal in directing liver injury progression due to the resultant liver inflammation, leading to fibrosis (3). To date, the precise etiology of AIH remains largely unknown; thus, the treatment of AIH poses a great challenge for physicians (4). Clinically, the current therapeutic options available for AIH mainly consist of various immunosuppressive agents (4), whereas the therapeutic efficacy of immunosuppressive agents is limited. Patients with AIH are unable to obtain long-term histological remission only by receiving immunosuppressive treatment (5). Furthermore, some patients with AIH still respond insufficiently to immunosuppressive agents, presenting with a prolonged course and repeated onset (1). Additionally, the adverse side-effects of immunosuppressive agents appear inevitable (6). Therefore, the identification of novel effective drugs which can be used to prevent the progression of AIH is of utmost importance.

Correspondence to: Professor Mei Liu, Department of Gastroenterology, Tongji Hospital of Tongji Medical College, Huazhong University of Science and Technology, Wuhan, Hubei 430030, P.R. China
E-mail: fliumei@126.com

Abbreviations: SOP, sophoricoside; AIH, autoimmune hepatitis; ALT, alanine aminotransferase; AST, aspartate aminotransferase; ConA, concanavalin-A; LPS, lipopolysaccharide; NAFLD, non-alcoholic fatty liver disease; ROS, reactive oxygen species; pCYP2D6, plasmid CYP2D6; 8-OHDG, 8-hydroxy-2-deoxyguanosine; MDA, malondialdehyde; T-AOC, total antioxidant capacity; GSH-Px, glutathione peroxidase; SEM, standard error of the mean; ANOVA, one-way analysis of variance; TCM, traditional Chinese medicine

Key words: autoimmune hepatitis, sophoricoside, antioxidative activity, NF-κB signaling pathway, network pharmacology

Chinese herbal medicines are considered penitential therapeutic agents for AIH and have unique advantages in the treatment of hepatic fibrosis (7). Sophoricoside (SOP) is an isoflavone glycoside extracted from the dried fruit of *Sophora japonica* L., which belongs to the traditional Chinese herb (8). Previous studies using animal experiments have revealed that SOP exerts therapeutic effects on non-alcoholic fatty liver disease (NAFLD), allergic asthma, dermatitis and lipopolysaccharide (LPS)-induced lung injury (9-12). The pharmacological properties of SOP reported thus far include the modulation of lipogenesis, anticancer, immune regulation and antioxidant effects (9-12). However, the pharmacological effects and regulatory mechanisms of SOP have not yet been explored in AIH or in autoimmune diseases.

In the present study, a mouse model of AIH was established to evaluate the effects of SOP on AIH. A mouse model of concanavalin A (ConA)-induced hepatitis was also used, as this model is commonly used in the study of AIH (13). However, the liver injury induced by ConA developed rapidly and could not fully mimic the chronic progression of AIH in the human body. Moreover, the acute liver injury induced by ConA exhibited a self-healing tendency, which usually disappeared after 48 h. Furthermore, the specific autoantibodies against liver, tissue fibrosis and the characteristic features of hepatic pathology could not be detected in ConA-induced AIH (13). Cytochrome P450 2D6 (CYP2D6) is a recognized human autoantigen in type-2 AIH and the adenovirus expressing human CYP2D6 was first used in an attempt to establish a mouse model of chronic AIH by Holdener *et al* (14). Based on previous research, an improved chronic CYP2D6-AIH mouse model was established by repeated injections of the human CYP2D6 expression plasmid targeting the liver (15). This model of CYP2D6-induced AIH can well resemble the chronic pathological process of AIH *in vivo,* and chronic inflammation, liver fibrosis and autoantibodies against the liver, characteristic of hepatic pathology can all be detected in this model mouse (15). Herein, the pharmacological effects and regulatory mechanisms of SOP in AIH were explored in the improved CYP2D6-AIH mouse model in combination with the ConA-induced acute immune-mediated liver injury model.

The present study demonstrates that SOP exerts therapeutic effects against autoimmune-mediated hepatic damage in mice. It is demonstrated that mechanistically, SOP attenuates liver inflammation and fibrosis via the inhibition of oxidative stress and NF-κB signaling pathway activation in hepatocytes.

Materials and methods

Animals and experimental protocol. Specific pathogen-free C57BL/6 male mice (n=48, 6-8 weeks old, weighing 20-25 g) were purchased from GemPharmatech Co., Ltd. The mice were housed in the specific pathogen-free environment at 24±2˚C with an alternating 12 h light/dark cycle and allowed free access to food and water at the Laboratory Animal Center of Tongji Hospital of Tongji Medical College. All experimental protocols were conducted following the Chinese National Guidelines for ethical review of animal welfare (GB/T 35892-2018) and approved by the Ethics Committee of Animal Experiments of Tongji Hospital, Tongji Medical College, Huazhong University of Science and Technology (approval no. TJH-202104021).

Establishment of moue model of AIH and drug administration. The mouse model of chronic CYP2D6-AIH was established by an adenovirus infection first and followed by a repeated tail vein injection of the CYP2D6 overexpression plasmid (pCYP2D6, 60 μg per injection) on days 1, 4, 9, 13, 17, 21, 25, as previously described (15). SOP (cat. no. HY-N0423; $C_{21}H_{20}O_{10}$, purity >99%) was purchased from MedChemExpress. For research on the improved chronic CYP2D6-AIH mouse model, the mice were randomly divided into four groups as follows: The CON group (n=6), SOP group (n=6), AIH group (n=6) and SOP + AIH group (n=6). SOP was administered by intraperitoneal injection once daily (30 mg/kg) from the 13th day. The detailed experimental protocol for each group is illustrated in Fig. 1A.

For research using the mouse model of ConA-induced acute hepatitis, the mice were randomly divided into the normal CON group (n=6), SOP group (n=6), ConA group (n=6) and SOP + ConA group (n=6). The mice were injected with a single dose of ConA (15 mg/kg, cat. no. L7647, MilliporeSigma) via the tail vein to induce acute autoimmune-mediated liver injury, as previously described (16). The mice were treated with SOP 3 days prior to the ConA injection. The treatment scheme of each group is presented in Fig. 1B.

At the endpoint of the experiment, the mice were anesthetized with pentobarbital sodium (70 mg/kg, administered intraperitoneally) for the harvest of blood from the orbital sinus and were sacrificed subsequently by cervical vertebra dislocation. Immediately following sacrifice, liver specimens were collected. Part of the livers were fixed in 4% paraformaldehyde solution and the remaining parts were preserved at -80˚C.

Network pharmacology. The two-dimensional structure of SOP was obtained from the PubChem database. The potential target genes of SOP were retrieved from online databases, including traditional Chinese medicine (TCM) systems pharmacology (TCMSP) (https://tcmsp-e.com/tcmsp.php) and PharmMapper (http://lilab-ecust.cn/pharmmapper/index.html), and the duplicates of two databases were removed. To collect the common targets of SOP on AIH, 'autoimmune hepatitis' was used as the key word for searching in the GeneCards database. The intersection between SOP targets and AIH-related genes was then screened out using an online Venn diagram tool (http://www.ehbio.com/test/venn/).

Protein-protein interaction (PPI) target network. The intersection targets between SOP targets and AIH-related genes were input into the STRING database (http://string-db.org/) to construct a PPI network. Cytoscape software 3.6.0 (http://www.cytoscape.org) was used to visualize the network and underwent the calculation of topological parameters. The top 10 common targets were selected according to the degree and above-average betweenness centrality (17).

Enrichment analysis. To predict the underlying regulatory mechanisms of SOP in AIH, the Gene Ontology (GO) biological functional enrichment and Kyoto Encyclopedia

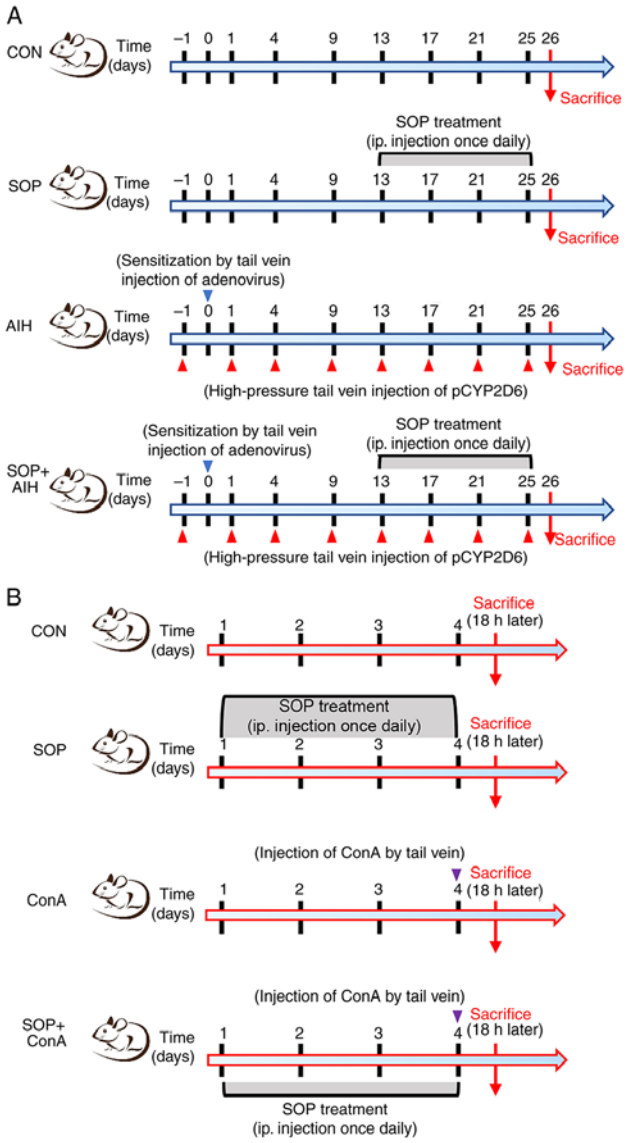

Figure 1. Animal model and experimental design. (A) Schematic diagram of the improved chronic CYP2D6-AIH mouse model and intervention. Mice were first sensitized by an adenovirus infection via tail vein injection on day 0, and received a rapid tail vein injection of pCYP2D6 (60 μg per injection) regularly. SOP was administered by intraperitoneal injection once daily (30 mg/kg) on day 13. (B) Schematic diagram of the mouse model of ConA-induced acute liver injury and the intervention. Mice were injected with ConA (15 mg/kg) via the tail vein and sacrificed after 18 h. CYP2D6, cytochrome P450 2D6; SOP, sophoricoside; CON, control.

of Genes and Genomes (KEGG) signaling pathway enrichment analysis was performed using the DAVID database (https://david.ncifcrf.gov/tools.jsp). The GO biological functional enrichment analysis consists of biological processes (GO_BP), cellular components (GO_CC) and molecular function (GO_MF) analysis. The enrichment analysis of target genes in Transcription Factor Targets was performed using the Metascape database (http://metascape.org).

Cells, cell culture and drug intervention. The AML12 cell lines were kept in the Institute of Liver and Gastrointestinal Diseases (Tongji Hospital, Huazhong University of Science and Technology). The AML12 cells were cultured in DMEM/F12 medium with 10% fetal bovine serum (Invitrogen; Thermo Fisher Scientific, Inc.), 1% insulin-transferrin-selenium solution [cat. no. 60708ES10, Yeasen Biotechnology (Shanghai) Co., Ltd.] and 40 ng/ml dexamethasone (cat. no. HY-14648, MedChemExpress). The cells were incubated at 37˚C in 5% CO_2, as previously described (18). After the AML12 cells were cultured until they adhered to the wells, LPS (cat. no. L4391, MilliporeSigma) was added at a concentration of 1,000 ng/ml for 24 h. To explore the *in vitro* effects of SOP, the AML12 cells were treated with SOP at 50 and 100 μM for 24 h prior to LPS stimulation.

Biochemistry measurements. The venous blood of mice was collected and centrifuged (3,000 x g, 10 min, at 4˚C). The supernatants were submitted to the Clinical Laboratory of Tongji Hospital (Wuhan, China) to measure the level of transaminase including alanine aminotransferase (ALT) and aspartate aminotransferase (AST).

For the detection of malondialdehyde (MDA), total antioxidant capacity (T-AOC) and glutathione peroxidase (GSH-Px) levels in mouse liver tissue and AML12 cells, the lysates sample were first collected by repeated ultrasonic spallation, and was measured using the malondialdehyde assay kit (cat. no. A003-1-2, Nanjing Jiancheng Taihao Biotechnology Co., Ltd.), total antioxidant capacity assay kit (cat. no. A015-2-1, Nanjing Jiancheng Taihao Biotechnology Co., Ltd.) and Glutathione Peroxidase assay kit (cat. no. A006-2-1, Nanjing Jiancheng Taihao Biotechnology Co., Ltd.), respectively, according to the manufacturer's instructions.

Histopathological analysis and immunohistochemistry. The livers were carefully isolated from the mice, fixed in a 4% paraformaldehyde solution (at least 24 h at 25˚C), and subsequently embedded in paraffin, and cut to yield 3-μm-thick sections. The sliced sections were stained with hematoxylin and eosin (H&E solution; 4 min at 25˚C) and Sirius red (20 min at 25˚C) to evaluate liver inflammation and fibrosis, respectively. The stains and fixative used, and technical support for H&E and Sirius staining were supplied by the Hubei Bios Biological Technology Co., Ltd. Images of H&E and Sirius staining were obtained using an inverted-phase contrast microscope (Olympus Corporation).

For immunohistochemistry, following dewaxing in xylene, rehydration in ethanol and antigen retrieval, the sliced sections were incubated with the 8-hydroxy-2-deoxyguanosine (8-OHDG; 1:100; cat. no sc-393871, Santa Cruz Biotechnology, Inc.) or phosphorylated (p-)p65 NF-κB (1:100; cat. no. 13346, Cell Signaling Technology, Inc.) primary antibodies overnight at 4˚C. The following day, the sliced sections were incubated with horseradish peroxidase-conjugated polyclonal goat anti-rabbit secondary antibodies (1:200; cat. no. AS014, ABclonal) for 1 h at room temperature. Finally, the sections were visualized with DAB and hematoxylin (Hubei Bios Biological Technology Co., Ltd.) using inverted phase contrast microscope (Olympus Corporation), as previously described (19).

RNA extraction and reverse transcription-quantitative PCR (RT-qPCR). Total RNA was extracted from the liver tissue or AML12 cells using the MolPure TRleasy Plus Total RNA kit [cat. no. 19211ES60, Yeasen Biotechnology

(Shanghai) Co., Ltd.]. Complementary DNA (cDNA) was synthesized using HiScript II Q RT SuperMix for qPCR (cat. no. R222-01, Nanjing Vazyme Biotech Co., Ltd.). The quantification of target mRNA was performed using ChamQ Universal SYBR qPCR Master Mix (cat. no. Q711-02, Nanjing Vazyme Biotech Co., Ltd.) on an ABI StepOne Real-Time PCR system (Thermo Fisher Scientific, Inc.). qPCR was performed under the following conditions: Initial denaturation at 95˚C for 3 min, followed by 45 cycles at 95˚C for 5 sec and 60˚C for 30 sec, and a final step at 95˚C for 5 sec and 60˚C for 1 min. The expression levels of mRNAs were normalized to GAPDH expression, and the $2^{-\Delta\Delta Cq}$ method was used to calculate the expression levels (19,20). All primers were synthesized by Beijing Tsingke Biological Technology, Co. Ltd., and are listed in Table SI.

Protein extraction and western blot analysis. Liver tissue or AML12 cells were collected and placed in RIPA Lysis Buffer (cat. no. 2002, Wuhan Servicebio Technology Co., Ltd.) containing a cocktail of protease inhibitors, homogenized on ice, and centrifugated at 12,000 x g, 4˚C for 15 min. The supernatant was collected and the protein concentration was measured using a BCA kit (cat. no. 2026-200T, Wuhan Servicebio Technology Co., Ltd.). A total of 40 μg protein per well was electrophoresed on 10% SDS polyacrylamide gel. The protein bands were then transferred onto PVDF membranes (MilliporeSigma). The PVDF membranes were then blocked with 5% non-fat milk for 1 h at room temperature and incubated with the primary antibodies overnight at 4˚C. The following antibodies were used: p-p65 NF-κB (1:1,000; cat. no. 13346; Cell Signaling Technology, Inc.), p65 NF-κB (1:1,000; cat. no. 8242; Cell Signaling Technology, Inc.), β-actin (1:5,000; cat. no. 66009-1-Ig; Proteintech Group, Inc.), TNF-α (1:1,000; cat. no. 60291-1-Ig; Proteintech Group, Inc.), IFN-γ (1:1,000; cat. no. 15365-1-AP; Proteintech Group, Inc.), IL-1β (1:1,000; cat. no. 16806-1-AP; Proteintech), IL-6 (1:1,000; cat. no. A0286; ABclonal), followed by incubation with goat anti-mouse IgG (H+L)-HRP (1:2,000; cat. no. SA00001-1; Proteintech Group, Inc.) or goat anti-rabbit IgG (H+L)-HRP (1:2,000; cat. no. SA00001-2; Proteintech Group, Inc.) for 1 h at room temperature. The blots referred to the expression of the antibody-linked protein was visualized by enhanced chemiluminescence using an ECL assay kit (cat. no. E412-01, Nanjing Vazyme Biotech Co., Ltd.). Image J software (version 1.50i; National Institutes of Health) was used to quantify the protein bands intensity.

Cell viability assay. The AML12 cells were uniformly seeded in 96-well plates at a density of 5,000 cells per well. Following treatment with various concentrations of SOP (50, 100 and 200 μM) for 48 h, the viability of the cells in each group was detected using the Cell Counting Kit (CCK-8) assay [10 μl CCK-8 per well, cat. no. 30203ES60, Yeasen Biotechnology (Shanghai) Co., Ltd.]. The cell viability was reflected by the absorbance value at 450 nm, and was measured using a microplate reader (BioTek Instruments, Inc.).

Measurement of reactive oxygen species (ROS) levels. The AML12 cells were uniformly seeded in six-well plates and incubated with 10 μM H_2DCFDA (cat. no. HY-D0940, MedChemExpress) for 30 min at 37˚C, and the fluorescence intensity of the cells subjected to the different treatments was then evaluated using a fluorescence microscope (Olympus Corporation).

Immunofluorescence staining assay. The cells were sequentially fixed in 4% paraformaldehyde solution, permeabilized in 0.3% Triton-X, blocked by 10% goat serum, and incubated with p65 NF-κB antibody (1:100; cat. no. 8242; Cell Signaling Technology, Inc.) at 4˚C overnight. The following day, the cells were incubated with CY3-conjugated goat anti-rabbit IgG (1:200; cat. no. BA1032, Boster Bio) for 1 h at room temperature. Images were recorded using an inverted fluorescence phase contrast microscope (Olympus Corporation).

Statistical analysis. The resulting data are presented as the mean ± standard error of the mean (SEM). Statistical analysis was performed using GraphPad Prism software version 6.0 (GraphPad Software, Inc.). The differences between groups were compared using the non-parametric one-way analysis of variance (ANOVA) followed by Tukey's post hoc tests. A value of $P<0.05$ was considered to indicate a statistically significant difference. All experiments were repeated at least three times.

Results

Key targets of SOP in AIH. The two-dimensional structure of SOP is presented in Fig. 2A. To identify the potential target genes of SOP, network pharmacological analysis was performed using the TCMSP database. After removing the duplicates, a total of 294 target genes of SOP were screened out. Moreover, through the GeneCards database, 1,427 AIH-related genes were obtained by using the quartile relevance score as the cut-off. The SOP targets were then intersected with the AIH-related targets. Finally, a total of 103 commonly matched targets were obtained (Fig. 2B). To explore the association among these targets, a PPI network was established using the STRING database, and the topological parameters, including the closeness centrality, between centrality and degree centrality were calculated (Fig. 2C). The top 10 key targets of SOP against AIH were selected for subsequent analyses (Fig. 2C and Table SII).

Potential mechanisms underlying the effects of SOP on AIH. To explore the underlying regulatory mechanisms of SOP in AIH, the selected top 10 common target genes were subjected to GO and KEGG enrichment analyses using the DAVID database. Based on the significance level, the top 20 significantly enriched terms were selected and are exhibited in Fig. 3A-D, respectively. By taking a comprehensive view of the enriched terms, it was noted that the enriched terms associated with the metabolism of ROS were highly ranked in all categories of enrichment analysis. In the GO_BP enrichment analysis, the results revealed that SOP was involved in the regulation of cellular response to ROS (Fig. 3A). The mitochondrion, which was the primary source of ROS in cells, was the top two cellular components influenced by SOP (Fig. 3B). The results of GO_MF analysis revealed that SOP was related to a series of reactions related to ROS production, including nitric-oxide

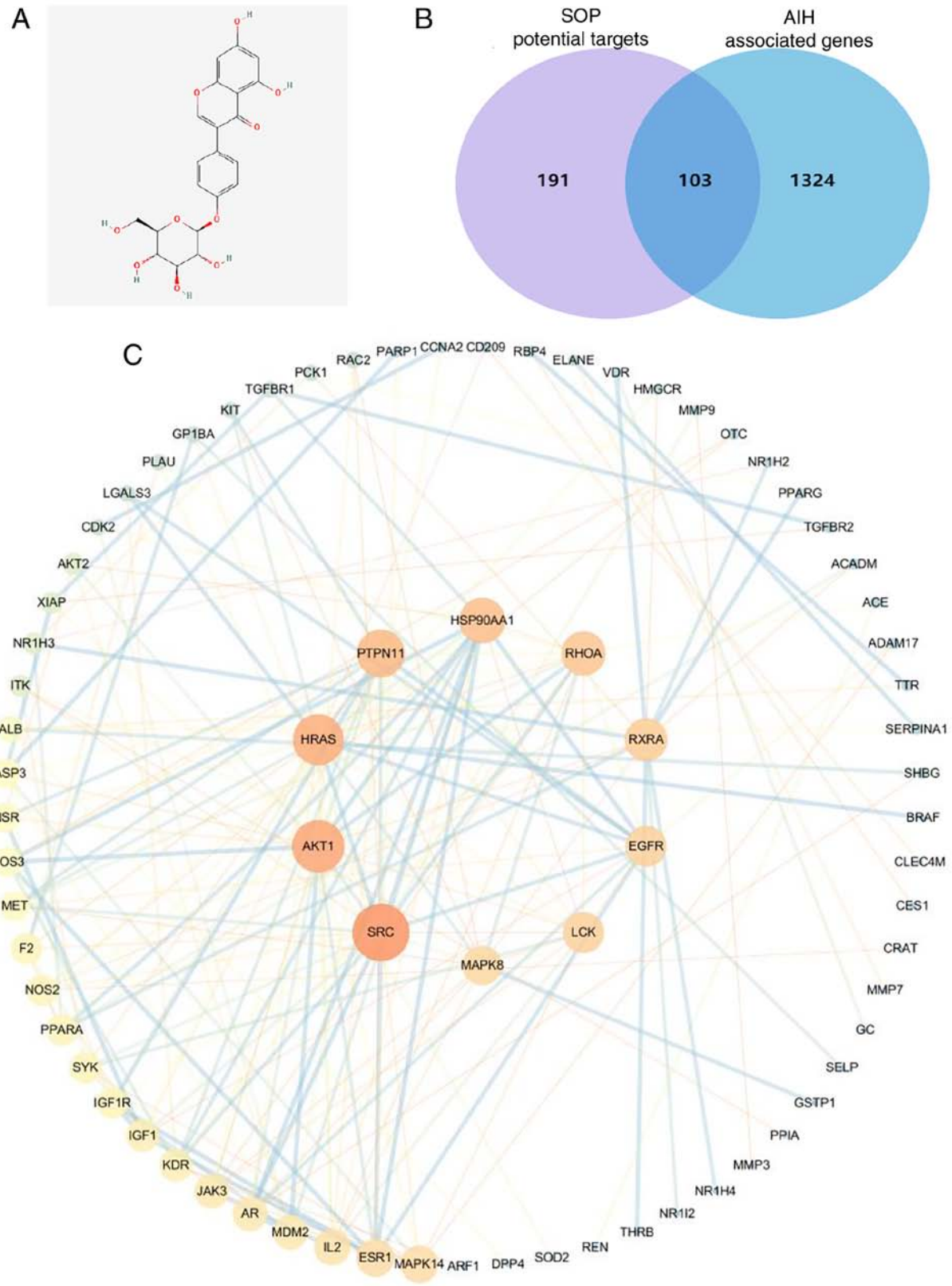

Figure 2. Network pharmacology analysis of the effects of SOP on AIH. (A) Two-dimensional chemical structure of SOP. (B) Venn diagram of 103 common targets between predicted targets of SOP and genes associated with AIH in the GeneCards database. (C) Protein-protein interactions network schematic of intersection targets of SOP and AIH. The warm color tone and node size denote a higher degree, and the thick dark-colored lines denote closer structure linkage. SOP, sophoricoside; AIH, autoimmune hepatitis.

synthase regulator activity, ATP binding and ATPase binding (Fig. 3C). Moreover, the results of KEGG enrichment analysis suggested that SOP participated in the chemical carcinogenesis by affecting ROS (Fig. 3D). In general, the data from GO and KEGG enrichment analyses predicted that the effects of SOP on AIH were mainly exerted by regulating oxidative stress.

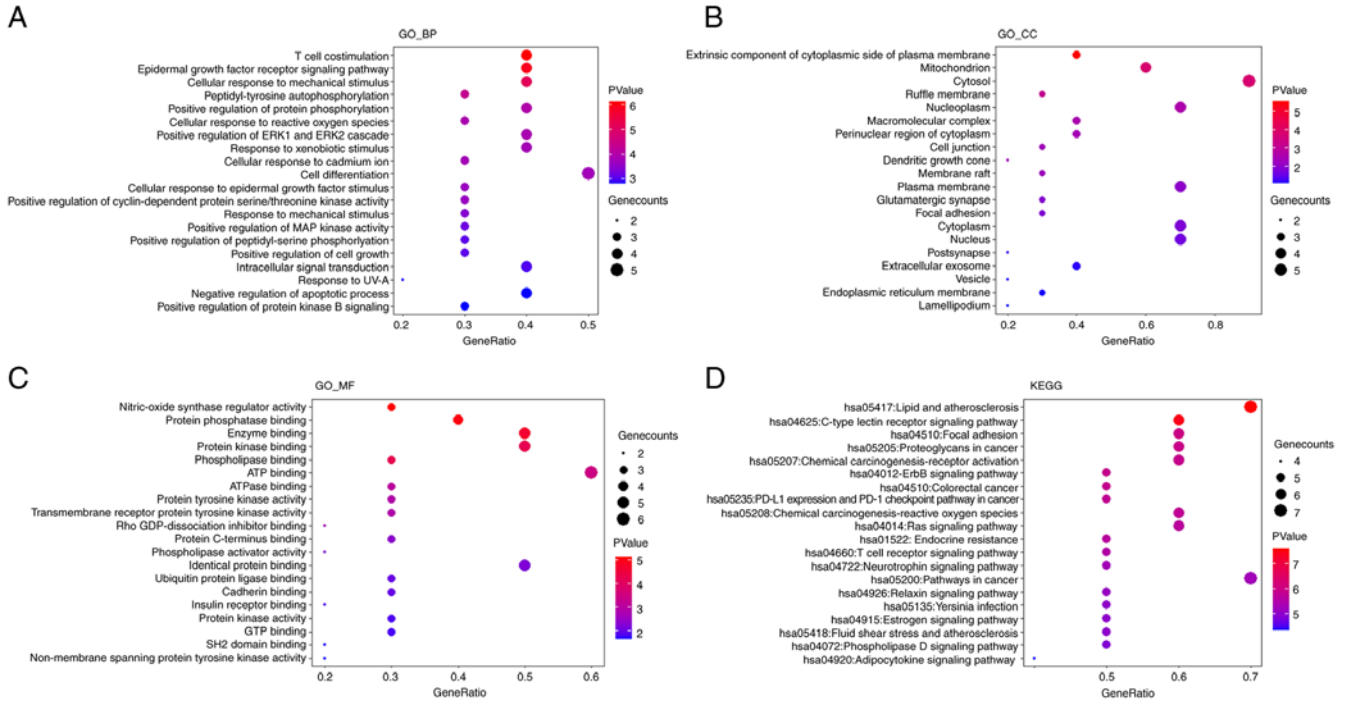

Figure 3. Bioinformatics analysis of the effects of SOP on AIH. The terms (A) biological processes, (B) cellular components, and (C) molecular function in GO enrichment analysis of the top 10 intersected targets between SOP targets and AIH-related genes. (D) KEGG enrichment analysis of the top 10 common targets from the network. SOP, sophoricoside; AIH, autoimmune hepatitis; GO, Gene Ontology; KEGG, Kyoto Encyclopedia of Genes and Genomes; BP, biological process; CC, cellular component; MF, molecular function.

SOP treatment attenuates autoimmune-mediated liver injury in an improved chronic AIH mouse model. To further confirm the effects of SOP treatment on AIH, an improved autoimmune-mediated hepatitis model was adopted, namely the CYP2D6-AIH mouse model. SOP was administered daily at a dose of 30 mg/kg (intraperitoneally). At the endpoint of the experiment, compared with the CON group, mice from the AIH group manifested evident pathological changes of AIH, including an elevation in the levels of serum liver enzymes, enhanced inflammatory cytokine production, interface hepatitis and tissue fibrosis (Fig. 4A-D). After almost 2 weeks of SOP treatment, the elevation in the levels of serum ALT/AST in AIH mice decreased significantly (Fig. 4A). The results of H&E staining revealed that in the mice with AIH treated with SOP, the histological damage was attenuated in contrast to that of the mice from the AIH group (Fig. 4B). Consistent with the results of histological analysis, the enhanced production of inflammatory cytokines in the mice with AIH was significantly suppressed by SOP administration (Fig. 4C and D). Moreover, the mice from the SOP + AIH group exhibited markedly attenuated liver fibrosis compared to the AIH group mice (Fig. 4E).

SOP treatment suppresses hepatocyte oxidative stress in mice with AIH and in LPS-stimulated AML12 cells. As mentioned above, bioinformatics analysis predicted that the major biological process in the pathogenesis of AIH targeted by SOP was oxidative stress, which is characterized by excessive ROS production. Considering that the distressed hepatocytes are the key source of ROS in the liver (21), several indices reflecting the degree of oxidative stress in hepatocytes were evaluated. Hepatocyte injury in the mouse liver induced by ROS in the present study was detected by examining the level of 8-OHDG, which is commonly used as a marker of oxidative damage. According to the data, following SOP treatment, the elevation in the levels of hepatic MDA in mice with chronic AIH was significantly decreased (Fig. 5A), and the overall decreased hepatic antioxidant ability in mice with AIH measured by T-AOC and GSH-Px exhibited a considerable enhancement (Fig. 5B and C). The oxidative damage to mouse liver cells induced by ROS was further assessed by immunohistochemical staining with 8-OHDG. The results revealed that compared with the mice from the CON group, oxidative damage to hepatocytes was enhanced in mice from the AIH group, while mice from the SOP + AIH group exhibited alleviated hepatic oxidative damage compared with the AIH group (Fig. 5D). The results of *in vitro* experiments revealed that treatment with SOP significantly reversed the excessive increase in MDA levels in AML12 cells induced by LPS (Fig. 5E), and upregulated the low levels of T-AOC and GSH-Px in a concentration-dependent manner (Fig. 5F and G). Moreover, it was observed that the level of ROS in AML12 cells extensively increased following LPS stimulation and decreased in cells pre-treated with SOP (Fig. 5H). These results indicated that SOP treatment exerted hepatoprotective effects by eliminating ROS in hepatocytes and promoting the antioxidant defense mechanisms.

SOP treatment suppresses the activation of the NF-κB signaling pathway in mice with AIH and in LPS-stimulated AML12 cells. Through enrichment analysis of the key target genes in Transcription Factor Targets, it was identified that the targets of SOP were primarily regulated by the gene set NF-κB (GO: M12240) (Fig. 6A). According to the *in vivo* experimental

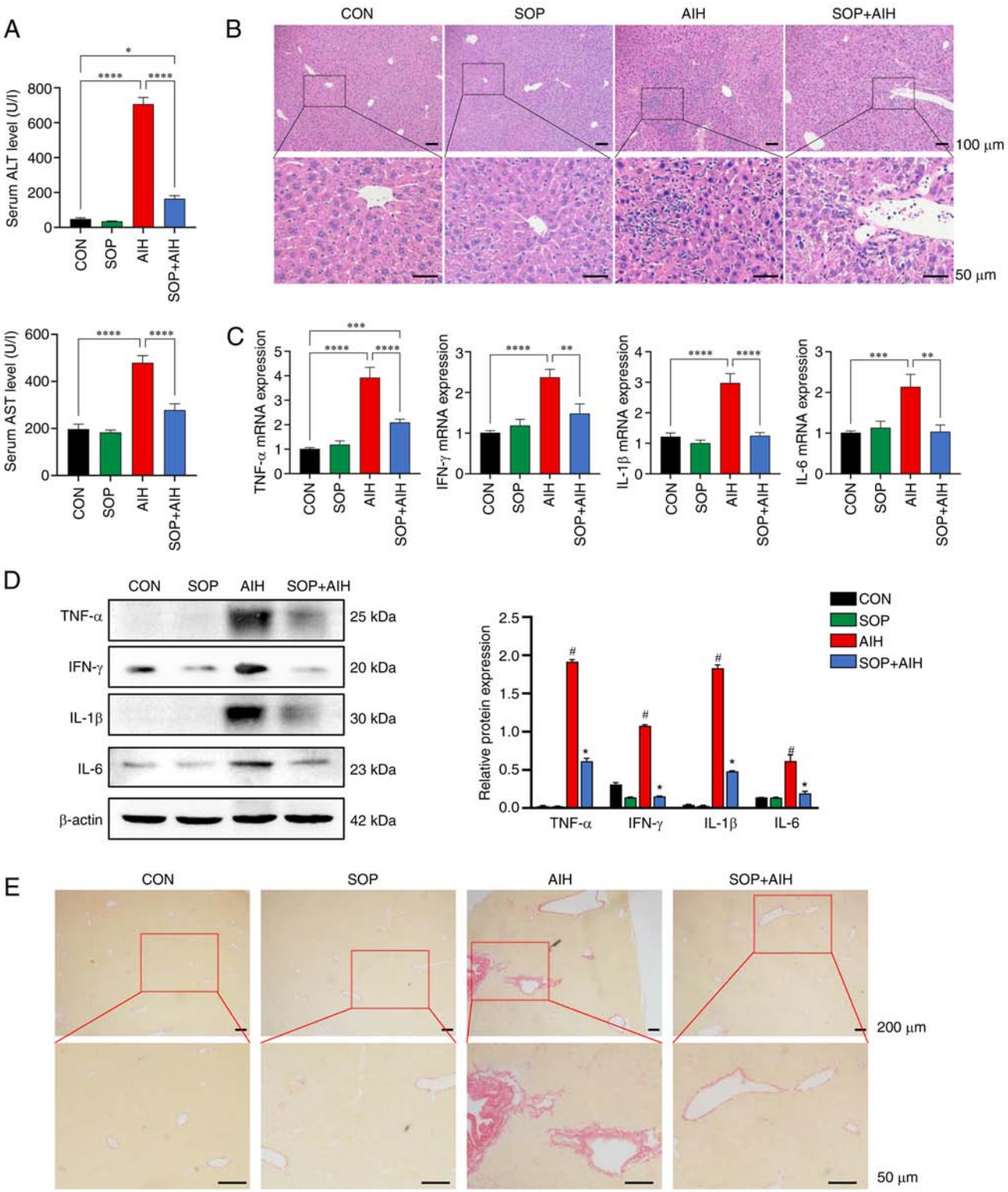

Figure 4. SOP treatment attenuates hepatic inflammation and fibrosis in an improved mouse model of chronic AIH. (A) Serum levels of ALT (top panel) and AST (bottom panel) in mice. (B) Hematoxylin and eosin staining of liver tissues (upper panels: Magnification x100; scale bars, 100 μm; bottom panels: Magnification, x400; scale bars, 50 μm). The relative expression levels of inflammatory cytokines in the liver were analyzed using (C) reverse transcription PCR and (D) western blot analysis. (E) Sirius red staining of mouse liver tissues. (upper panels: Magnification, x40; scale bars, 200 μm; bottom panels: Magnification, x200; scale bars, 50 μm). The data represent the mean ± SEM, n=6 per group. (A-C) *P<0.05, **P<0.01, ***P<0.001 and ****P<0.0001. (D) $^{\#}$P<0.05, between the AIH and CON group; *P<0.05 between the SOP + AIH and AIH group. SOP, sophoricoside; AIH, autoimmune hepatitis; CON, control; ALT, alanine aminotransferase; AST, aspartate aminotransferase.

data, the activation of the NF-κB signaling pathway in the liver was enhanced in mice with AIH. The results of western blot analysis indicated that the mice with AIH treated with SOP exhibited a decreased activation of the NF-κB signaling pathway compared to the mice in the AIH group (Fig. 6B). Immunohistochemical staining further confirmed that the

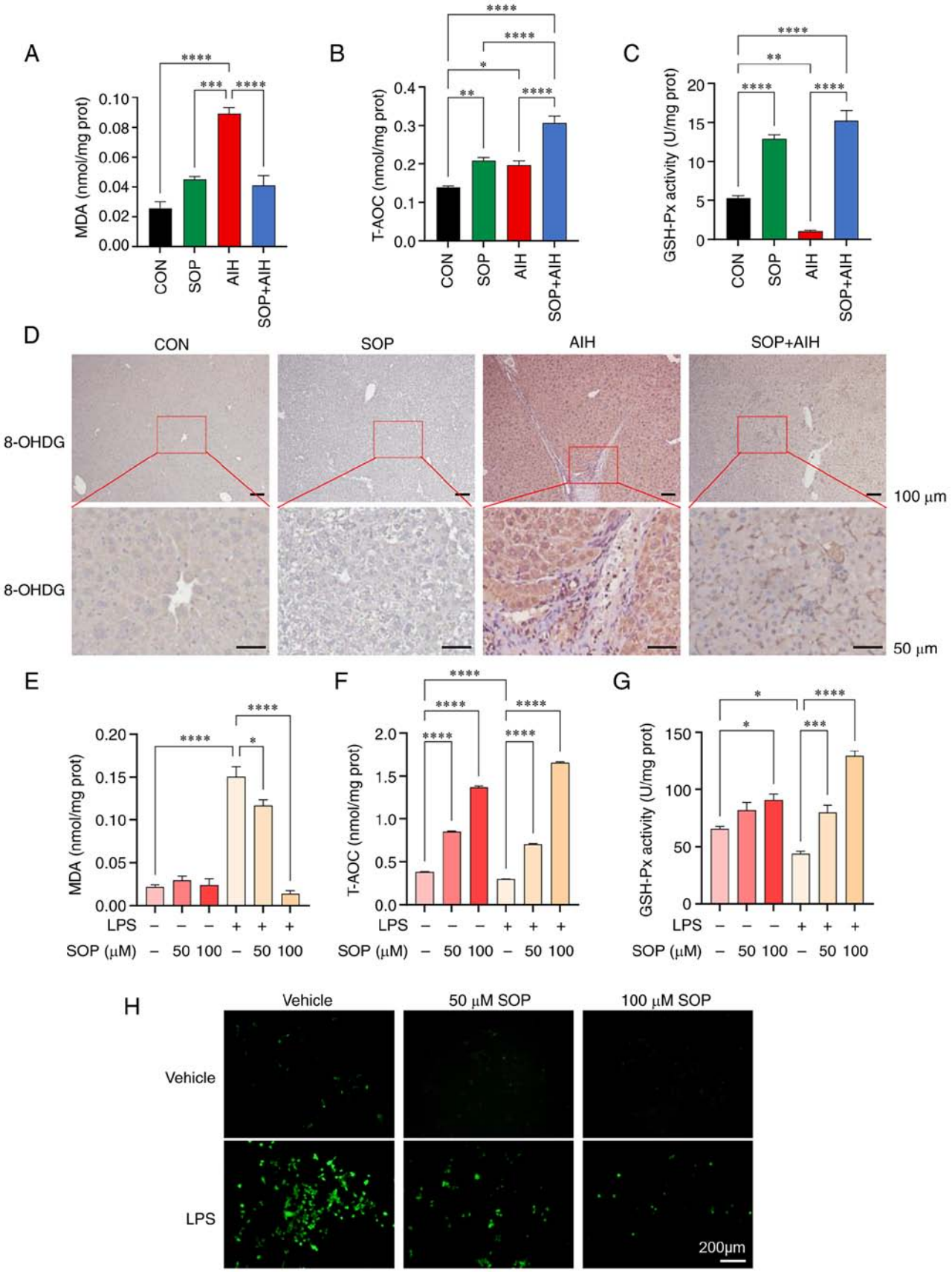

Figure 5. SOP treatment inhibits hepatocellular oxidative stress in a mouse model of chronic AIH and in LPS-stimulated AML12 cells. (A) Lysates of mouse liver tissue were collected for the detection of (A) MDA, (B) T-AOC, and (C) GSH-Px. (D) Representative images of immunostaining for the ROS marker, 8-OHDG, in the liver. AML12 cells were treated with SOP at 50 and 100 μM with or without LPS (1,000 ng/ml) for 24 h. Cell lysates were collected for the detection of (E) MDA, (F) T-AOC, and (G) GSH-Px. (H) Fluorescence microscopic images of ROS level in AML12 cells treated with SOP at 50 and 100 μM with or without LPS (1,000 ng/ml) for 24 h. *P<0.05, **P<0.01, ***P<0.001 and ****P<0.0001. SOP, sophoricoside; AIH, autoimmune hepatitis; CON, control; LPS, lipopolysaccharide; 8-OHDG, 8-hydroxy-2-deoxyguanosine; MDA, malondialdehyde; T-AOC, total antioxidant capacity; GSH-Px, glutathione peroxidase.

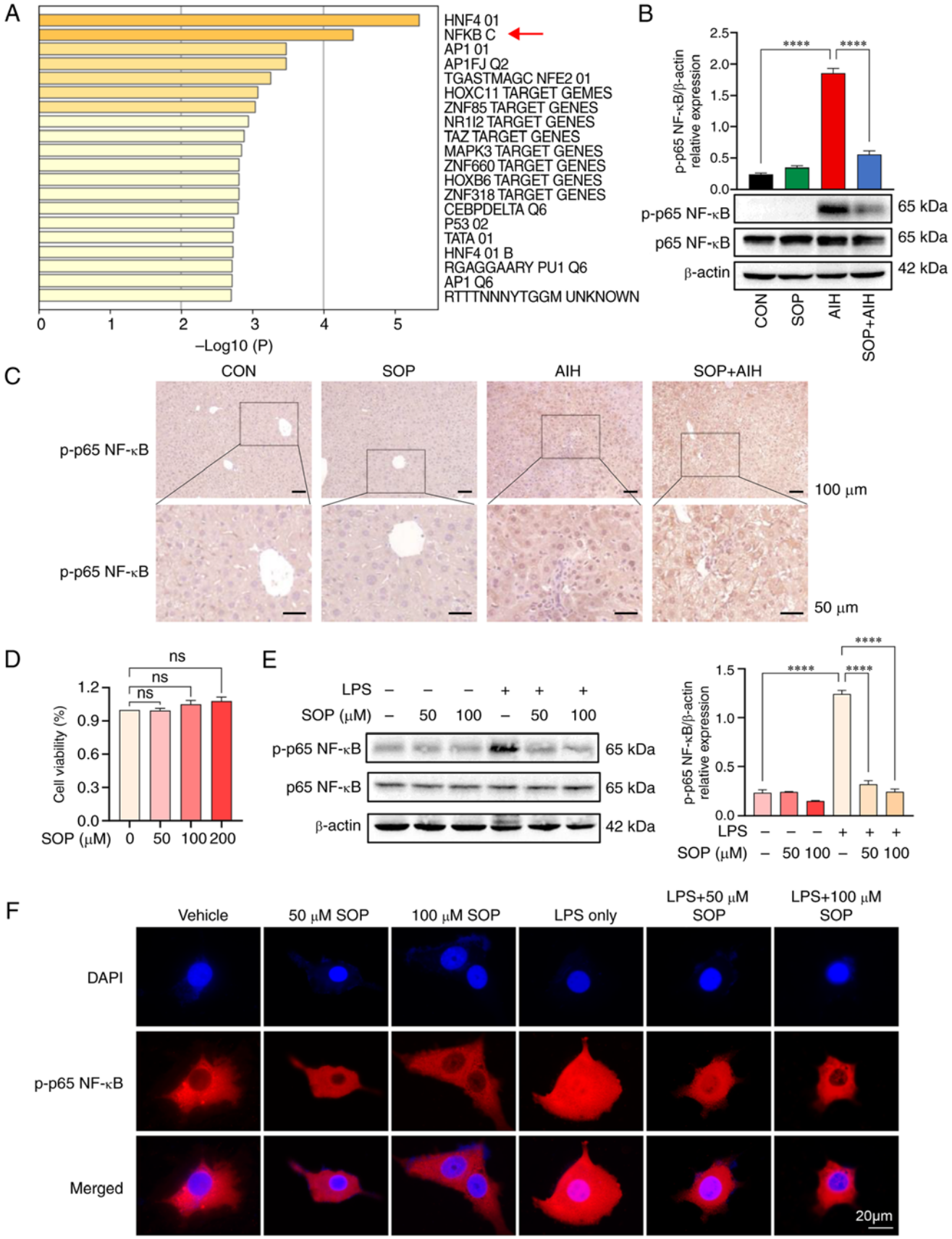

Figure 6. The activation of the NF-κB signaling pathway in mice with AIH and in LPS-stimulated AML12 cells is suppressed by SOP treatment. (A) The enrichment analysis in Transcription Factor Targets of common targets between predicted SOP and AIH-related genes targets. (B) Western blot analysis of NF-κB protein expression in mouse liver. (C) Representative images of immunostaining for p-p65 NF-κB in the liver. (D) The cell viability of AML12 cells treated with SOP at 0, 50, 100 and 200 μM for 48 h. (E) AML12 cells were pre-treated with SOP at 50 and 100 μM with or without LPS (1,000 ng/ml) for 24 h. Cell lysates were collected for the determination of NF-κB protein expression using western blot analysis. (F) Cells were stained with anti-p65 NF-κB (red) and DAPI (blue) and immunofluorescence images were obtained by confocal microscopy. ****P<0.0001. ns, not significant; SOP, sophoricoside; AIH, autoimmune hepatitis; CON, control; LPS, lipopolysaccharide.

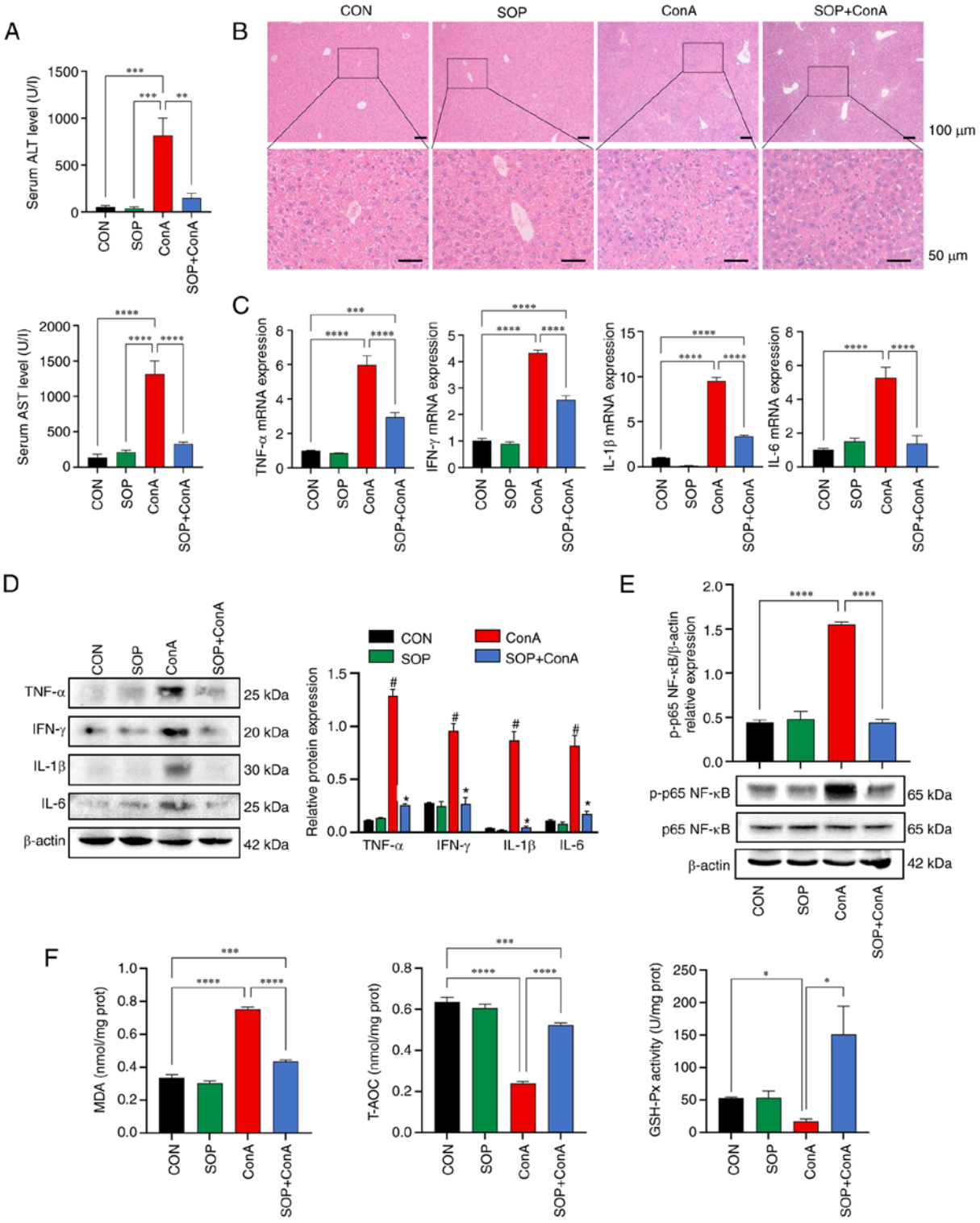

Figure 7. The ConA-induced hepatitis was alleviated in SOP-treated mice accompanied by reduced oxidative stress and NF-κB activation in the liver. (A) Quantification of serum ALT and AST levels in mice. (B) The histology of mouse hepatic tissue was assessed using hematoxylin and eosin staining. (C) The mRNA expression levels of TNF-α, IFN-γ, IL-1β and IL-6 in mouse liver tissues were measured using reverse transcription-quantitative PCR. (D) The protein expression levels of TNF-α, IFN-γ, IL-1β and IL-6 in mouse liver tissues were detected using western blot analysis. (E) Western blot analysis of NF-κB activation in liver tissue. (F) Lysates of mouse liver tissue were collected for the detection of MDA, T-AOC and GSH-Px. *P<0.05, **P<0.01, ***P<0.001 and ****P<0.0001. (D) $^{\#}$P<0.05, between the ConA and CON group; *P<0.05, between the SOP + ConA and ConA group. ConA, concanavalin-A; SOP, sophoricoside; AIH, autoimmune hepatitis; CON, control; ALT, alanine aminotransferase; AST, aspartate aminotransferase; MDA, malondialdehyde; T-AOC, total antioxidant capacity; GSH-Px, glutathione peroxidase.

increased protein expression of p-p65 NF-κB in the liver cells of mice with AIH was decreased by SOP treatment (Fig. 6C). In addition, the effects of SOP treatment on the NF-κB signaling pathway were further investigated *in vitro*. Firstly, the potential cytotoxicity of SOP on AML12 cells was evaluated by CCK-8 assay after the AML12 cells were incubated with

SOP for 48 h. The results indicated no cellular toxicity of SOP against the AML12 cells at concentrations ranging from 50 to 200 μM (Fig. 6D). Cell lysates were collected and the content of p-p65/p65 NF-κB protein was detected using western blot analysis. It was found that the relative protein expression of p-p65 NF-κB was upregulated in the LPS-stimulated AML12 cells and was subsequently suppressed by SOP treatment (Fig. 6E). Simultaneously, the results of immunofluorescence staining revealed that the LPS-induced nuclear translocation of p65 NF-κB in the AML12 cells was significantly blocked by SOP treatment (Fig. 6F). These data suggested that SOP treatment blocked the activation of the NF-κB signaling pathway in hepatocytes.

SOP treatment inhibits oxidative stress and NF-κB activation in mice with ConA-induced hepatitis. To further examine the protective effects of SOP against autoimmune-mediated liver injury, the ConA-induced acute AIH mouse model was additionally adopted to assess the grade of oxidative stress and NF-κB activation in the mouse liver before and after SOP treatment. According to the results obtained, the mice from the ConA group presented with elevated serum levels of ALT/AST, increased inflammatory cytokine expression levels and interface hepatitis. Compared with the ConA group mice, the SOP + ConA group mice exhibited significantly lower serum levels of ALT/AST and inflammatory cytokine expression levels, as well as an alleviated pathophysiological damage in the liver (Fig. 7A-D). Furthermore, the results of western blot analysis revealed that the ConA-induced enhancement of p-p65 NF-κB protein expression in the mouse liver was significantly suppressed by SOP administration (Fig. 7E). Additionally, mice with ConA-induced liver injury exhibited increased levels of MDA, and decreased T-AOC and GSH-Px levels; these effects were partially restored in mice treated with SOP (Fig. 7F).

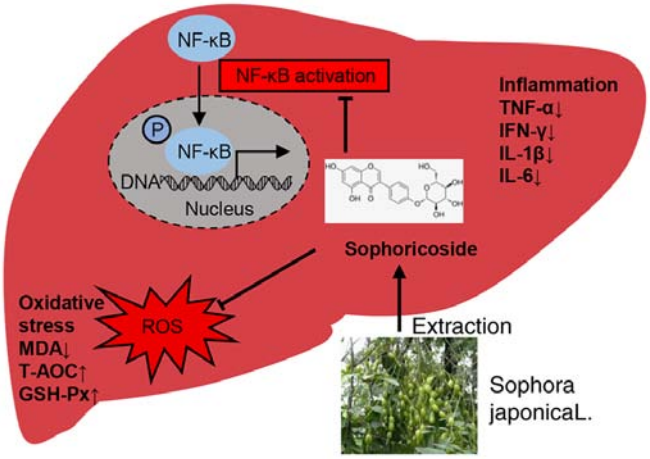

Figure 8. Schematic diagram of the therapeutic mechanisms of SOP on autoimmune-mediated hepatic damage. SOP ameliorates autoimmune-mediated hepatitis via inhibition of oxidative stress and NF-κB signaling pathway activation in hepatocytes. SOP, sophoricoside; MDA, malondialdehyde; T-AOC, total antioxidant capacity; GSH-Px, glutathione peroxidase; ROS, reactive oxygen species.

Discussion

AIH is characterized by autoimmune-mediated inflammatory damage to the liver with a chronic course (22). Due to the complex etiology of AIH, there are currently no effective drugs available with which to reduce hepatic fibrosis and achieve histological remission in patients with AIH (22). Therefore, the exploration of novel drugs for AIH is still essential. TCM includes a diverse selection of agents which can be used for human healthcare. SOP is a bioactive component of the Chinese herbal medicine, *Sophora japonica* L. (8). In the present study, it was found that SOP attenuated chronic and acute autoimmune-mediated liver injury by suppressing oxidative stress and the NF-κB signaling pathway activation in liver cells.

The pathophysiological mechanisms of AIH are complex. There is evidence to indicate that a number of factors, such as immune disorder, oxidative stress, the dysregulation of immune-related signaling pathways and intestinal dysbiosis, can contribute to the development of AIH and destroy hepatocytes (23-25). In light of the complex factors involved in the pathogenesis of AIH, herein, network pharmacology was performed to predict which of these pathophysiological mechanisms in AIH are regulated by SOP. Network pharmacology is a platform utilized to predict the molecular targets and regulatory mechanisms, as well as components of TCM for disease (26). In a comprehensive view of the network pharmacological results, it was noted that the modulation of oxidative stress may be a key mechanism associated with the benefits of SOP in AIH. Based on the top 20 significantly enriched terms, it was found that cellular response to ROS was respectively the second and the ninth significant term in GO_BP and KEGG enrichment analysis. Following the GO_CC enrichment analysis, the second significant term was mitochondrion, which is the major source of cellular ROS (27). The GO_MF analysis also revealed that SOP mainly influenced the process of cellular respiration, including nitric-oxide synthase regulatory activity, ATP binding and ATPase binding (28). Therefore, it was anticipated that SOP mainly exerted effects on AIH by regulating oxidative stress.

The studies by Kim and Lee (9,10), Zhang *et al* (11), Wu *et al* (12), Gao *et al* (29) and Li and Lu (30) have confirmed that SOP treatment can exert therapeutic effects in a number of diseases, such as NAFLD, dermatitis, allergic asthma, LPS-induced lung injury, cardiac hypertrophy, fructose-induced liver injury (9-12,29,30). The results of the present study indicated that SOP treatment reduce the serum ALT/AST level and suppressed the expression of pro-inflammatory cytokines, including TNF-α, IFN-γ, IL-1β and IL-6 in the mouse model of AIH. Moreover, the histological findings revealed that hepatic inflammation and tissue fibrosis in chronic autoimmune-mediated hepatitis could be prevented by SOP treatment. The normalization of serum transaminase is considered a key marker of full biochemical remission in patients with AIH (31). In addition, high levels of TNF-α, IFN-γ, IL-1β and IL-6 are the major pathogenetic inflammatory cytokines in AIH (22,32). The extension of hepatic fibrosis may proceed to cirrhosis and liver failure, leading to the deterioration of the clinical outcomes of patients (31). Taken together, these data suggest that SOP treatment can improve chronic autoimmune-mediated liver injury.

Oxidative stress is characterized by the excessive production of ROS and has been implicated in the pathogenesis of AIH (33-35). The hepatocyte is the major cell population within the liver that generates ROS under conditions of stress (21). It has been suggested that patients with AIH tend to present an increased level of hepatic ROS (24). The redundant ROS induced by oxidative stress attacks the cellular membrane and disrupts mitochondrial function, resulting in the death of hepatocytes and in tissue fibrosis (36-38). Moreover, ROS may promote hepatic fibrosis by stimulating hepatic stellate cells (39,40). It has been reported that SOP can exert antioxidant pharmacological effects in the treatment of NAFLD and LPS-induced acute lung injury (11,12). Consistently, the results of the *in vivo* and *in vitro* experiments in the present study indicated that treatment with SOP reduced the MDA levels and ROS, and upregulated T-AOC and GSH-Px in hepatocytes subjected to immune-mediated injury. MDA is one of the peroxidation products of polyunsaturated fatty acids, which is the most commonly used marker of oxidant stress (41). T-AOC and GSH-Px are indexes that reflect the anti-oxidant capability of tissue (42). Therefore, these results further validate the prediction from network pharmacology that SOP treatment can protect against AIH through the inhibition of oxidative stress, accompanied by the decreased production and enhanced elimination of ROS in hepatocytes.

On the other hand, the present study suggested that SOP also attenuated autoimmune-mediated liver injury via the inhibition of the NF-κB signaling pathway in hepatocytes. The enrichment analysis in Transcription Factor Targets indicated that the majority of genes targeted by SOP were significantly regulated by the transcription factor, NF-κB. The experimental data supported this prediction, demonstrating that treatment with SOP reduced the enhanced nuclear translocation of NF-κB in LPS-stimulated AML12 cells and suppressed the activation of p65 NF-κB protein in the livers of mice with AIH. It has been demonstrated that the activation of the NF-κB signaling pathway is vital in the progression of inflammatory liver disease (43). Patients with AIH often present with increased levels of NF-κB-induced inflammatory cytokines, such as TNF-α, IFNγ, IL-1β and IL-6 (30). The blockade of the NF-κB-mediated inflammatory signaling pathway can alleviate liver inflammation (44). The data presented herein demonstrated that SOP treatment inhibited the activation of the NF-κB signaling pathway and reduced inflammatory cytokine levels in mice with AIH.

In order to further validate the effects of SOP treatment on AIH, the present study adopted a mouse model of ConA-induced hepatitis. The ConA model is a canonical animal model for AIH research, which is mediated by T-cells and characterized by acute autoimmune-mediated liver injury resembling AIH (45). The results revealed that the hepatic damage induced by ConA was ameliorated by SOP treatment. Mice in the ConA model treated with SOP exhibited decreased levels of oxidative stress and NF-κB activation in the liver. However, a limitation of the present study was that the role of the NF-κB signaling pathway during SOP treatment of AIH was not further verified by the overexpression of p-p65 NF-κB protein in mice with AIH treated with SOP. In addition, whether the NF-κB signaling pathway interacted with oxidative stress in the pathogenesis of AIH was not identified in the present study.

In conclusion, the present study demonstrates that SOP may have a potential therapeutic effect on AIH. Treatment with SOP can attenuate liver inflammation and prevent hepatic fibrosis progression in mice with chronic or acute autoimmune-mediated liver injury via the inhibition of oxidative stress and NF-κB signaling pathway activation in hepatocytes (Fig. 8).

Acknowledgements

Not applicable.

Funding

The present study was supported by grants from the National Natural Science Foundation of China (nos. 81974071 and 82270558).

Availability of data and materials

The datasets used and/or analyzed during the current study are available from the corresponding author on reasonable request.

Authors' contributions

YC and YL designed the study and wrote the manuscript. YC, LW, JX and SW performed all the experiments cooperatively. ZP and MY collected and analyzed the experimental data. FX and HW interpreted the experimental results and critically reviewed the manuscript. ML and DT conceived the study and supervised the study. All authors have read and approved the final manuscript. ML and DT confirm the authenticity of all the raw data.

Ethics approval and consent to participate

All experiments involving animals were conducted following the Chinese National Guidelines for ethical review of animal welfare (GB/T 35892-2018) and approved by the Ethics Committee of Animal Experiments of Tongji Hospital, Tongji Medical College, Huazhong University of Science and Technology (approval no. TJH-202104021).

Patient consent for publication

Not applicable.

Competing interests

The authors declare that they have no competing interests.

References

1. Mieli-Vergani G, Vergani D, Czaja AJ, Manns MP, Krawitt EL, Vierling JM, Lohse AW and Montano-Loza AJ: Autoimmune hepatitis. Nat Rev Dis Primers 4: 18017, 2018.
2. Floreani A, Restrepo-Jiménez P, Secchi MF, De Martin S, Leung PSC, Krawitt E, Bowlus CL, Gershwin ME and Anaya JM: Etiopathogenesis of autoimmune hepatitis. J Autoimmun 95: 133-143, 2018.

3. Sirbe C, Simu G, Szabo I, Grama A and Pop TL: Pathogenesis of autoimmune hepatitis-cellular and molecular mechanisms. Int J Mol Sci 22: 13578, 2021.
4. Manns MP, Lohse AW and Vergani D: Autoimmune hepatitis-update 2015. J Hepatol 62 (Suppl 1): S100-S111, 2015.
5. Expert Panel on Gastrointestinal Imaging; Hindman NM, Arif-Tiwari H, Kamel IR, Al-Refaie WB, Bartel TB, Cash BD, Chernyak V, Goldstein A, Grajo JR, *et al*: ACR appropriateness criteria® jaundice. J Am Coll Radiol 16: S126-S140, 2019.
6. Mack CL, Adams D, Assis DN, Kerkar N, Manns MP, Mayo MJ, Vierling JM, Alsawas M, Murad MH and Czaja AJ: Diagnosis and management of autoimmune hepatitis in adults and children: 2019 Practice guidance and guidelines from the American association for the study of liver diseases. Hepatology 72: 671-722, 2020.
7. Li H: Advances in anti hepatic fibrotic therapy with traditional Chinese medicine herbal formula. J Ethnopharmacol 251: 112442, 2020.
8. Chang L, Ren Y, Cao L, Sun Y, Sun Q, Sheng N, Yuan L, Zhi X and Zhang L: Simultaneous determination and pharmacokinetic study of six flavonoids from fructus sophorae extract in rat plasma by LC-MS/MS. J Chromatogr B Analyt Technol Biomed Life Sci 904: 59-64, 2012.
9. Kim BH and Lee S: Sophoricoside from styphnolobium japonicum improves experimental atopic dermatitis in mice. Phytomedicine 82: 153463, 2021.
10. Kim BH and Lee S: Sophoricoside from *Sophora japonica* ameliorates allergic asthma by preventing mast cell activation and $CD4^+$ T cell differentiation in ovalbumin-induced mice. Biomed Pharmacother 133: 111029, 2021.
11. Zhang Y, Li F, Jiang X, Jiang X, Wang Y, Zhang H, Zhang L, Fan S, Xin L, Yang B, *et al*: Sophoricoside is a selective LXRβ antagonist with potent therapeutic effects on hepatic steatosis of mice. Phytother Res 34: 3168-3179, 2020.
12. Wu YX, Zeng S, Wan BB, Wang YY, Sun HX, Liu G, Gao ZQ, Chen D, Chen YQ, Lu MD and Pang QF: Sophoricoside attenuates lipopolysaccharide-induced acute lung injury by activating the AMPK/Nrf2 signaling axis. Int Immunopharmacol 90: 107187, 2021.
13. Hao J, Sun W and Xu H: Pathogenesis of concanavalin A induced autoimmune hepatitis in mice. Int Immunopharmacol 102: 108411, 2022.
14. Holdener M, Hintermann E, Bayer M, Rhode A, Rodrigo E, Hintereder G, Johnson EF, Gonzalez FJ, Pfeilschifter J, Manns MP, *et al*: Breaking tolerance to the natural human liver autoantigen cytochrome P450 2D6 by virus infection. J Exp Med 205: 1409-1422, 2008.
15. Wang H, Yan W, Feng Z, Gao Y, Zhang L, Feng X and Tian D: Plasma proteomic analysis of autoimmune hepatitis in an improved AIH mouse model. J Transl Med 18: 3, 2020.
16. Wang S, Huang Z, Lei Y, Han X, Tian D, Gong J and Liu M: Celastrol alleviates autoimmune hepatitis through the PI3K/AKT signaling pathway based on network pharmacology and experiments. Front Pharmacol 13: 816350, 2022.
17. Lei Y, Wang S, Liu J, Yan W, Han P and Tian D: Identification of MCM family as potential therapeutic and prognostic targets for hepatocellular carcinoma based on bioinformatics and experiments. Life Sci 272: 119227, 2021.
18. Wang C, Li X, Zhang W, Liu W, Lv Z, Gui R, Li M, Li Y, Sun X, Liu P, *et al*: ETNPPL impairs autophagy through regulation of the ARG2-ROS signaling axis, contributing to palmitic acid-induced hepatic insulin resistance. Free Radic Biol Med 199: 126-140, 2023.
19. Lei Y, Han P, Chen Y, Wang H, Wang S, Wang M, Liu J, Yan W, Tian D and Liu M: Protein arginine methyltransferase 3 promotes glycolysis and hepatocellular carcinoma growth by enhancing arginine methylation of lactate dehydrogenase A. Clin Transl Med 12: e686, 2022.
20. Livak KJ and Schmittgen TD: Analysis of relative gene expression data using real-time quantitative PCR and the 2(-Delta Delta C(T)) method. Methods 25: 402-408, 2001.
21. Crosas-Molist E and Fabregat I: Role of NADPH oxidases in the redox biology of liver fibrosis. Redox Biol 6: 106-111, 2015.
22. Webb GJ, Hirschfield GM, Krawitt EL and Gershwin ME: Cellular and molecular mechanisms of autoimmune hepatitis. Annu Rev Pathol 13: 247-292, 2018.
23. Longhi MS, Mieli-Vergani G and Vergani D: Regulatory T cells in autoimmune hepatitis: An updated overview. J Autoimmun 119: 102619, 2021.
24. Kaffe ET, Rigopoulou EI, Koukoulis GK, Dalekos GN and Moulas AN: Oxidative stress and antioxidant status in patients with autoimmune liver diseases. Redox Rep 20: 33-41, 2015.
25. Wei Y, Li Y, Yan L, Sun C, Miao Q, Wang Q, Xiao X, Lian M, Li B, Chen Y, *et al*: Alterations of gut microbiome in autoimmune hepatitis. Gut 69: 569-577, 2020.
26. Wen Y, Han C, Liu T, Wang R, Cai W, Yang J, Liang G, Yao L, Shi N, Fu X, *et al*: Chaiqin chengqi decoction alleviates severity of acute pancreatitis via inhibition of TLR4 and NLRP3 inflammasome: Identification of bioactive ingredients via pharmacological sub-network analysis and experimental validation. Phytomedicine 79: 153328, 2020.
27. Oyewole AO and Birch-Machin MA: Mitochondria-targeted antioxidants. FASEB J 29: 4766-4771, 2015.
28. Maynard AG and Kanarek N: NADH ties one-carbon metabolism to cellular respiration. Cell Metab 31: 660-662, 2020.
29. Gao M, Hu F, Hu M, Hu Y, Shi H, Zhao GJ, Jian C, Ji YX, Zhang XJ, She ZG, *et al*: Sophoricoside ameliorates cardiac hypertrophy by activating AMPK/mTORC1-mediated autophagy. Biosci Rep 40: BSR20200661, 2020.
30. Li W and Lu Y: Hepatoprotective effects of sophoricoside against fructose-induced liver injury via regulating lipid metabolism, oxidation, and inflammation in mice. J Food Sci 83: 552-558, 2018.
31. European Association for the Study of the Liver: EASL clinical practice guidelines: Autoimmune hepatitis. J Hepatol 63: 971-1004, 2015.
32. Seki E and Schwabe RF: Hepatic inflammation and fibrosis: Functional links and key pathways. Hepatology 61: 1066-1079, 2015.
33. Sanz-Cameno P, Medina J, Garcia-Buey L, García-Sánchez A, Borque MJ, Martín-Vílchez S, Gamallo C, Jones EA and Moreno-Otero R: Enhanced intrahepatic inducible nitric oxide synthase expression and nitrotyrosine accumulation in primary biliary cirrhosis and autoimmune hepatitis. J Hepatol 37: 723-729, 2002.
34. Pemberton PW, Aboutwerat A, Smith A, Burrows PC, McMahon RF and Warnes TW: Oxidant stress in type I autoimmune hepatitis: The link between necroinflammation and fibrogenesis? Biochim Biophys Acta 1689: 182-189, 2004.
35. Beyazit Y, Kocak E, Tanoglu A and Kekilli M: Oxidative stress might play a role in low serum vitamin D associated liver fibrosis among patients with autoimmune hepatitis. Dig Dis Sci 60: 1106-1108, 2015.
36. Richter K, Konzack A, Pihlajaniemi T, Heljasvaara R and Kietzmann T: Redox-fibrosis: Impact of TGFβ1 on ROS generators, mediators and functional consequences. Redox Biol 6: 344-352, 2015.
37. Singh R and Czaja MJ: Regulation of hepatocyte apoptosis by oxidative stress. J Gastroenterol Hepatol 22 (Suppl 1): S45-S48, 2007.
38. Czaja AJ: Nature and implications of oxidative and nitrosative stresses in autoimmune hepatitis. Dig Dis Sci 61: 2784-2803, 2016.
39. Cui W, Matsuno K, Iwata K, Ibi M, Matsumoto M, Zhang J, Zhu K, Katsuyama M, Torok NJ and Yabe-Nishimura C: NOX1/nicotinamide adenine dinucleotide phosphate, reduced form (NADPH) oxidase promotes proliferation of stellate cells and aggravates liver fibrosis induced by bile duct ligation. Hepatology 54: 949-958, 2011.
40. Hernández-Gea V, Hilscher M, Rozenfeld R, Lim MP, Nieto N, Werner S, Devi LA and Friedman SL: Endoplasmic reticulum stress induces fibrogenic activity in hepatic stellate cells through autophagy. J Hepatol 59: 98-104, 2013.
41. Tsikas D: Assessment of lipid peroxidation by measuring malondialdehyde (MDA) and relatives in biological samples: Analytical and biological challenges. Anal Biochem 524: 13-30, 2017.
42. Dadheech G, Mishra S, Gautam S and Sharma P: Evaluation of antioxidant deficit in schizophrenia. Indian J Psychiatry 50: 16-20, 2008.
43. He G and Karin M: NF-κB and STAT3-key players in liver inflammation and cancer. Cell Res 21: 159-168, 2011.
44. Hoesel B and Schmid JA: The complexity of NF-κB signaling in inflammation and cancer. Mol Cancer 12: 86, 2013.
45. Liberal R, de Boer YS and Heneghan MA: Established and novel therapeutic options for autoimmune hepatitis. Lancet Gastroenterol Hepatol 6: 315-326, 2021.